SAND2019-2375C

Exceptional service in the national interest

Sandia National Laboratories

Device-level modeling of hole quantum dots in Ge

Mitchell Brickson[1,3], Andrew Baczewski[1], Will Hardy[2], Noah T. Jacobson[1], Tzu-Ming Lu[2], Leon Maurer[1], Dwight R. Luhman[2]

[1] Center for Computing Research, Sandia National Laboratories, Albuquerque, NM 87123, United States

[2] Sandia National Laboratories, Albuquerque, NM 87123, United States

[3] Center for Quantum Information and Control, University of New Mexico, Albuquerque, NM 87131, United States

U.S. DEPARTMENT OF ENERGY

NNSA National Nuclear Security Administration

This work was performed, in part, at the Center for Integrated Nanotechnologies, an Office of Science User Facility operated for the U.S. Department of Energy (DOE) Office of Science. Sandia National Laboratories is a multimission laboratory managed and operated by National Technology & Engineering Solutions of Sandia, LLC, a wholly owned subsidiary of Honeywell International Inc., for the U.S. Department of Energy's National Nuclear Security Administration under contract DE-NA0003525. SAND2019-?????

Modeling spin-orbit coupling in Ge

- Goal: understand electric dipole spin resonance (EDSR) experiments for Ge devices
- Approach: work with spin-orbit coupling (SOC) models to understand EDSR details
  - Simplest model:

$$\hat{H}_{so1} = i\alpha_1(\hat{\sigma}_- \otimes \hat{k}_+ - \hat{\sigma}_+ \otimes \hat{k}_-)$$

  - Expected form from $k \cdot p$-theory (E. Marcellina et al., Phys. Rev. B, 2017):

$$\hat{H}_{so3} = i\alpha_{3,1}\left(\hat{\sigma}_- \otimes \hat{k}_+^3 - \hat{\sigma}_+ \otimes \hat{k}_-^3\right) + i\alpha_{3,2}(\hat{\sigma}_- \otimes \hat{k}_-\hat{k}_+\hat{k}_- - \hat{\sigma}_+ \otimes \hat{k}_+\hat{k}_-\hat{k}_+)$$

- Developing a starting point for a full device-level model
  - Single-band effective mass theory for now; potentially misses important details (A. Mielnik-Pyszczorski et al., Scientific Reports, 2018)
  - Work toward a multi-band model that includes more parameters of Ge

Background

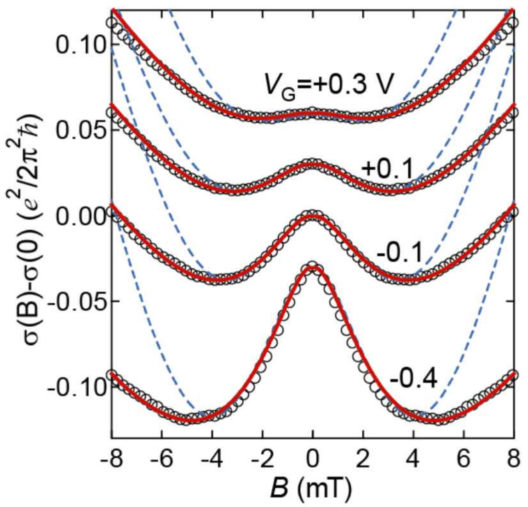

[1] R. Moriya et al., Phys. Rev. Lett. 2014

- Magnetoconductivity experiments (2DHGs), suggest SOC model better fits k^3 than k

- Theory calculations for Ge (and Si) holes based on $k \cdot p$-theory

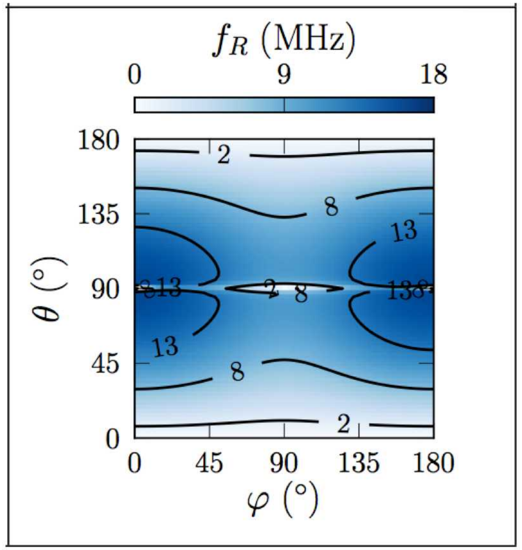

[2] B. Venitucci and Y. M. Niquet, arXiv preprint 2019

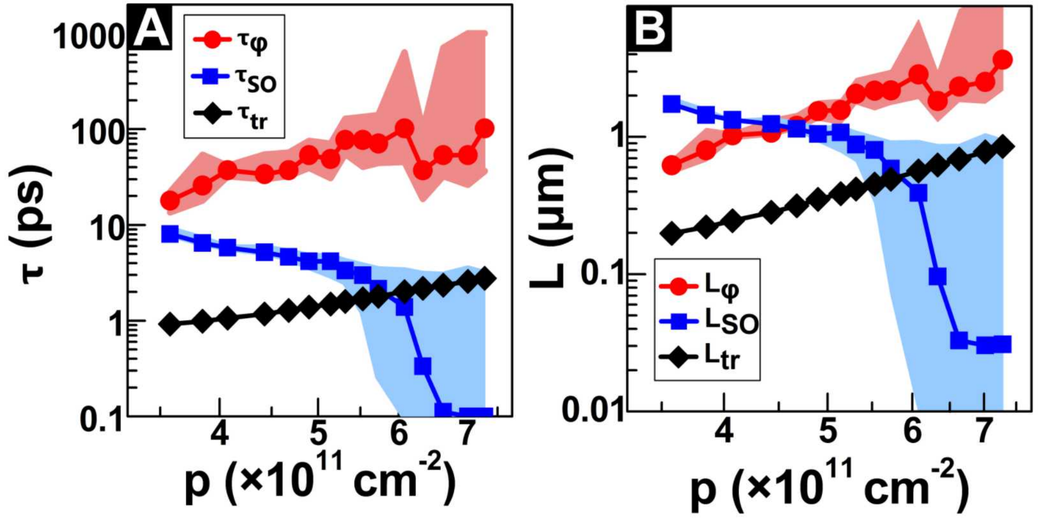

[3] C. T. Chou et al., Nanoscale 2018

- Magnetoconductivity experiments, fit model assuming SOC is k^3

- Experiments from 2DHGs suggest SOC is k^3 in Ge
- Open question for confined QDs

Workflow

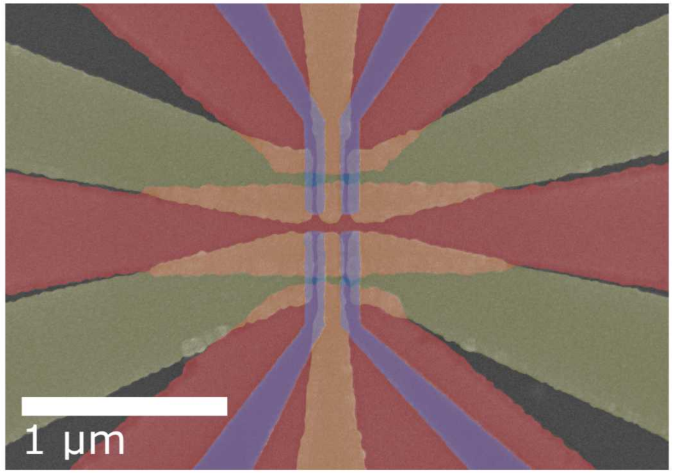

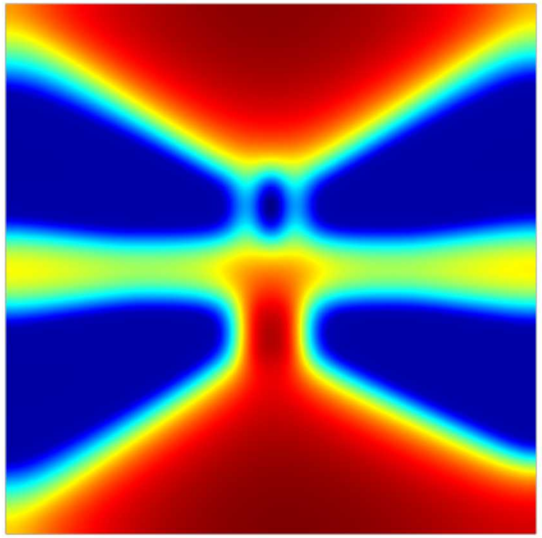

- Take gate layout and stack dimensions from device [1]
- Use Laconic [2] to calculate wavefunctions (w/o spin)

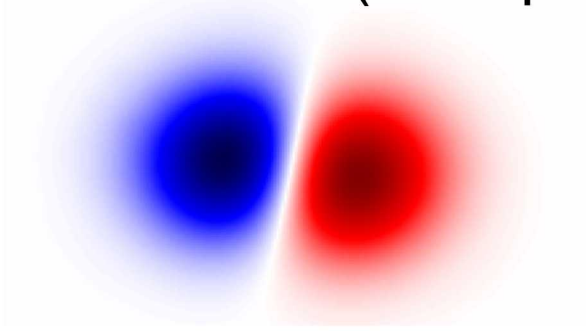

- Use COMSOL to calculate device potentials
- Use wavefunctions as a basis for calculations with spin

$$k_-^{\alpha\beta} = \langle\psi_\alpha|\hat{k}_-|\psi_\beta\rangle \rightarrow \hat{\sigma}_+ \otimes \hat{k}_-$$

[1] See Will Hardy's talk tomorrow, session L11.00005
[2] Sandia software, led by Andrew Baczewski

Modeling EDSR

- Compute change in potential for oscillations of middle gate
- Crystal axes determine SOC Hamiltonian
- Driving Hamiltonian:

$$\hat{H}_{ac} \sim V_{ac}\hat{y}$$

- Voltage oscillation: $1[mV]$, Applied B-field: $1[T]$
- Study Rabi frequency trends in SOC models

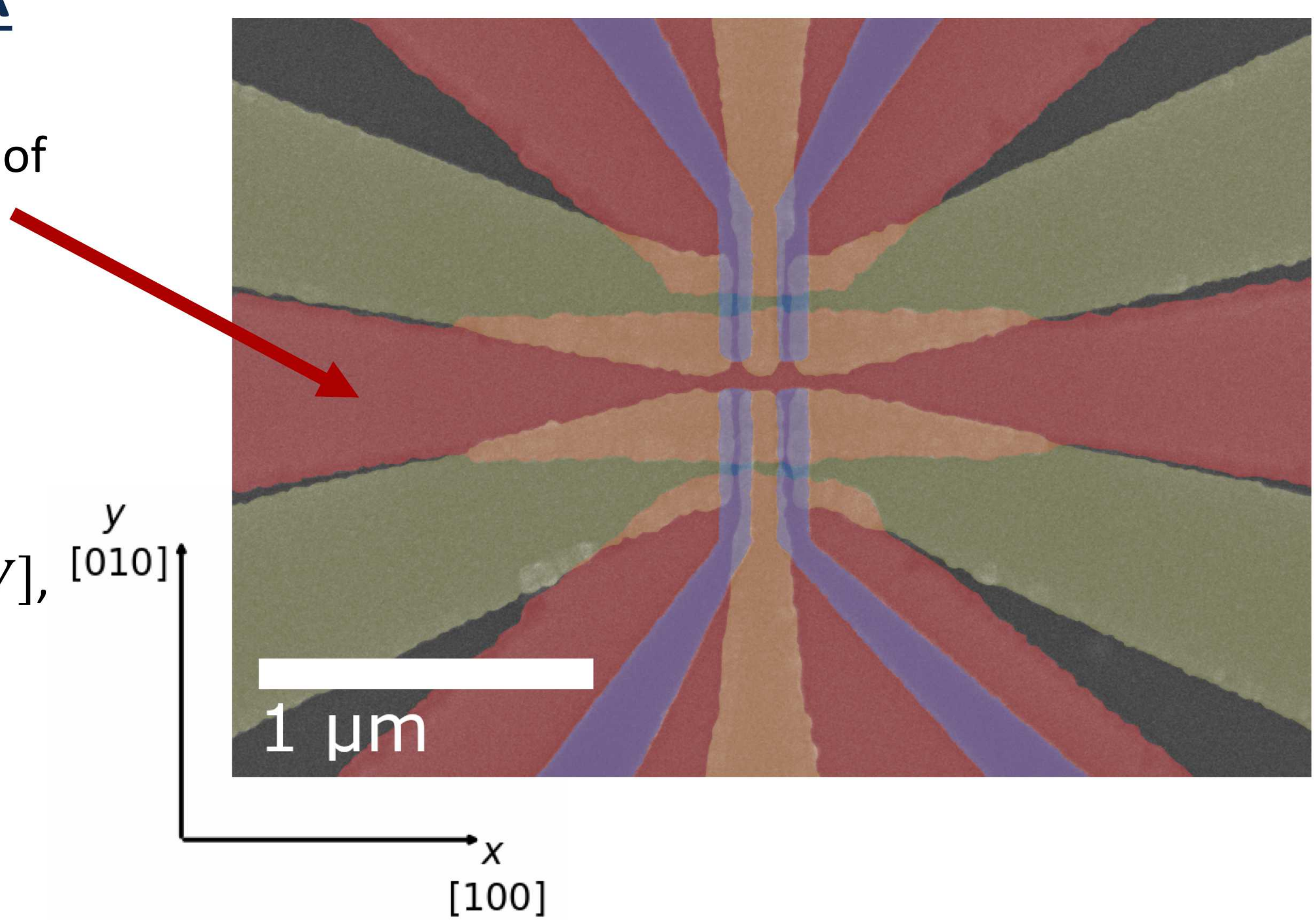

How we compute Rabi frequencies

- Full Hamiltonian:

$$\hat{H}_{full} = \hat{H}_k + \hat{H}_v + \hat{H}_{so} + \hat{H}_{ac}$$

kinetic part (includes B-field) — potential part — spin-orbit part — AC drive part

- Define basis states, $|\psi_j\rangle$, from the eigenstates of $\hat{H}_k + \hat{H}_v$, e.g.

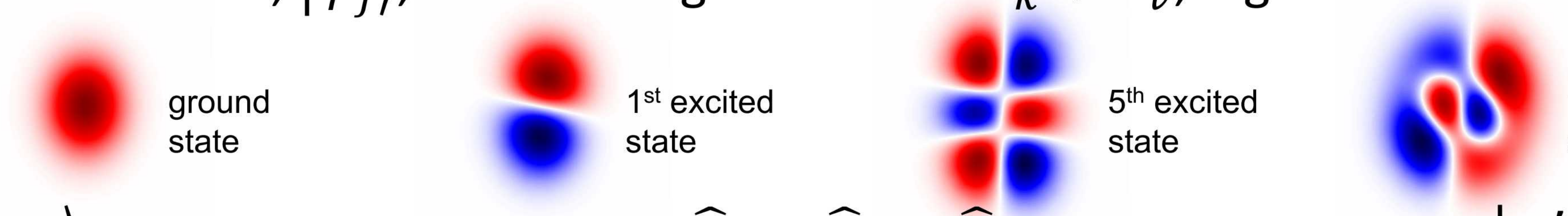

- Using $|\psi_j\rangle$s, expand and diagonalize $\hat{H}_k + \hat{H}_v + \hat{H}_{so}$ to get a new basis, $|\psi'_j\rangle$
- Calculate the Rabi frequency as

$$f_R = \frac{2\pi}{\hbar} \left| \langle \psi'_0 | \hat{H}_{ac} | \psi'_1 \rangle \right|$$

AC E-field along y → AC B-field along x

- Hamiltonian:

$$\hat{H}_{3,2} \approx \alpha_{3,2}(\hat{\sigma}_y \otimes (\hat{k}_x^2 + \hat{k}_y^2)\hat{k}_x - \hat{\sigma}_x \otimes (\hat{k}_x^2 + \hat{k}_y^2)\hat{k}_y)$$

- AC drive reduces Hamiltonian to effective magnetic field along x:

$$\hat{H}_{ac} \sim V_{ac}\hat{y} \;\; \rightarrow \;\; k_x \sim 0$$

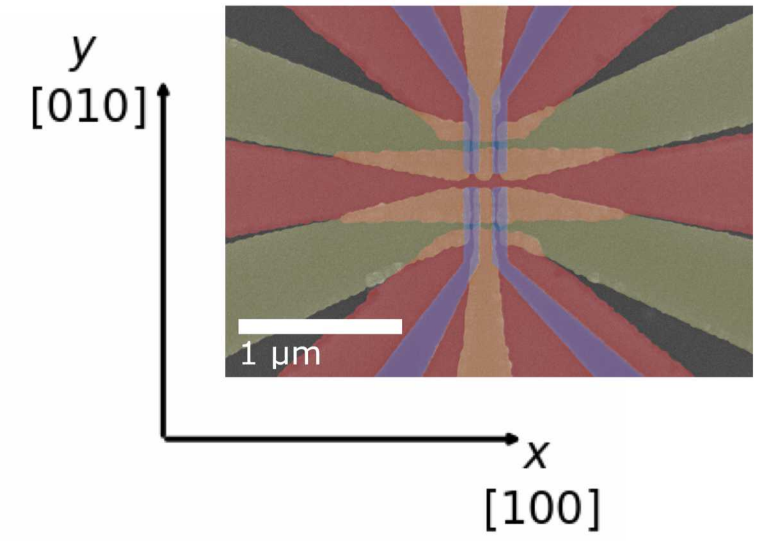

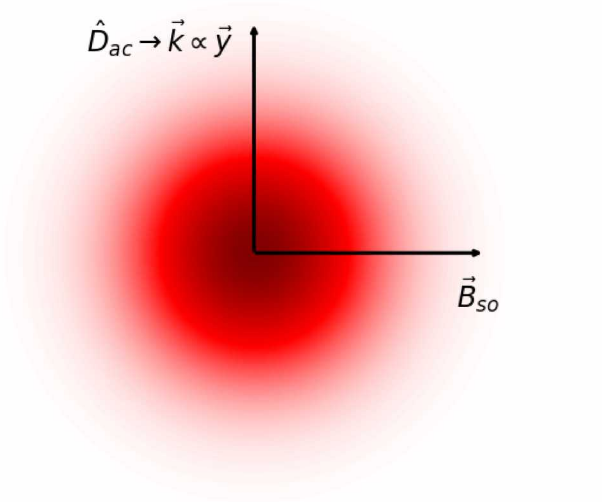

AC E-field along y → AC B-field along x

- Hamiltonian:

$$\hat{H}_{3,2} \approx \alpha_{3,2}\left(\cancel{\hat{\sigma}_y \otimes (\hat{k}_x^2 + \hat{k}_y^2)\hat{k}_x} - \hat{\sigma}_x \otimes (\hat{k}_x^2 + \hat{k}_y^2)\hat{k}_y\right)$$

- AC drive reduces Hamiltonian to effective magnetic field along x:

$$\hat{H}_{ac} \sim V_{ac}\hat{y} \;\rightarrow\; k_x \sim 0 \;\rightarrow\; \hat{H}_{3,2} \sim \hat{\sigma}_x \otimes (\hat{k}_x^2 + \hat{k}_y^2)\hat{k}_y \;\rightarrow\; \boldsymbol{B}_{so} \propto \vec{x}$$

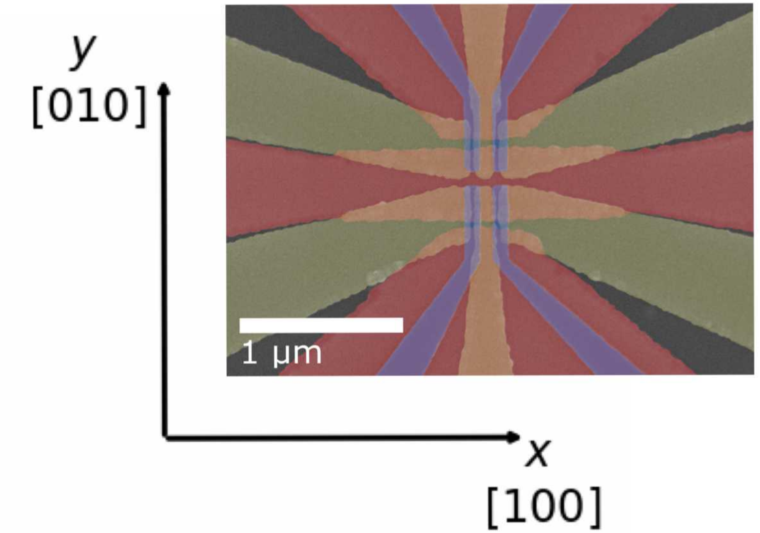

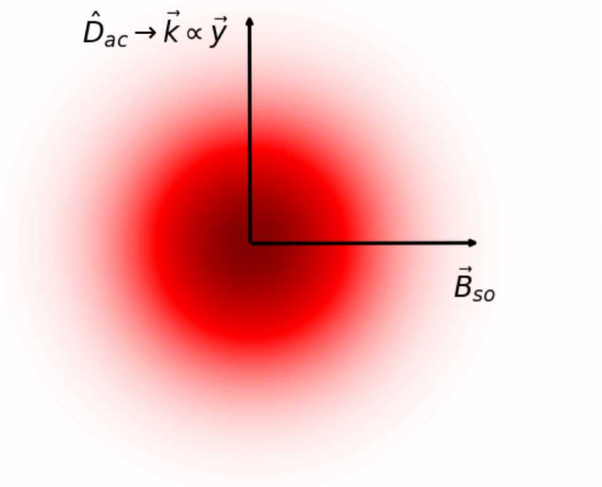

Strong rotations require orthogonal B-fields

- Should have weak rotations for

$$\boldsymbol{B}_{app} \parallel \boldsymbol{B}_{so}$$

- This fits the simulations:

$$f_R \propto |\boldsymbol{B}_{app} \times \boldsymbol{B}_{so}|$$

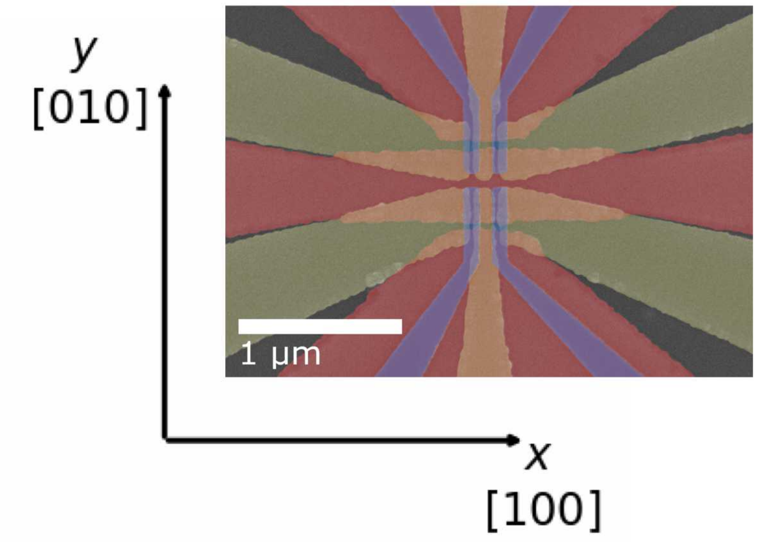

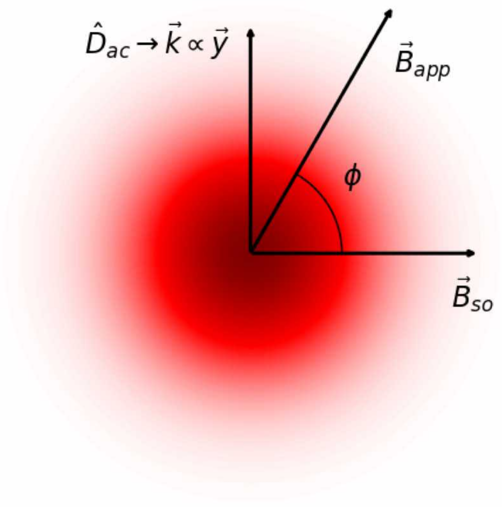

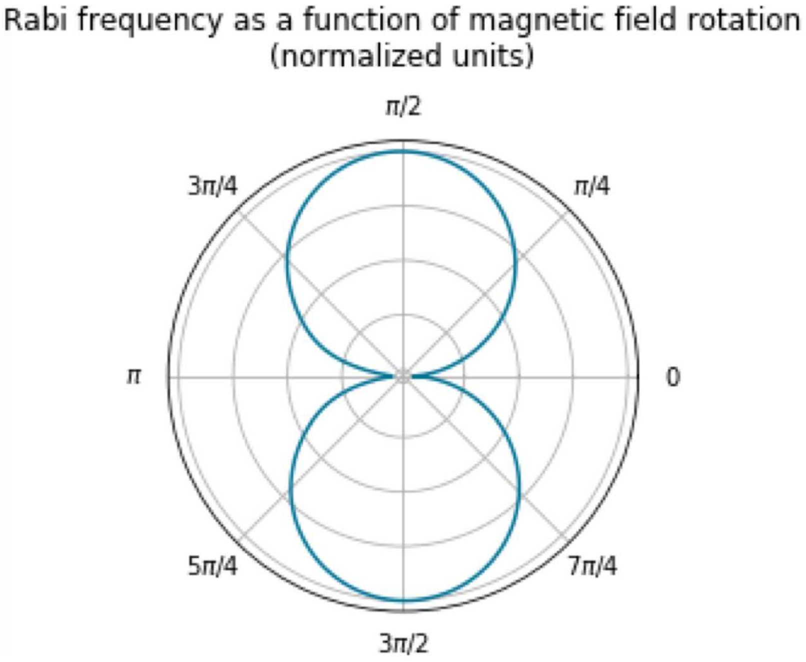

Importance of crystal axes to device design

- Coordinate system determines form of $\widehat{H}_{so3}$
  - $\hat{k}_x$ and $\hat{k}_y$ set by crystal axes
  - Rotation about the z-axis changes $\widehat{H}_{so3}$
- $\boldsymbol{B}_{so}$ is then a function of the crystal axes as well as the dipole perturbation
  - This adjusts the previous structure

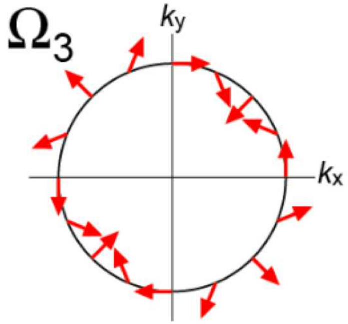

R. Moriya et al., PRL 2014

- Rotation of the spin-orbit field as a function of charge-carrier direction of motion for

$$\widehat{H}_{3,1} = i\alpha_{3,1}\left(\hat{\sigma}_- \otimes \hat{k}_+^3 - \hat{\sigma}_+ \otimes \hat{k}_-^3\right)$$

Importance of crystal axes to device design

- Coordinate system determines form of $\widehat{H}_{so3}$
  - $\hat{k}_x$ and $\hat{k}_y$ set by crystal axes
  - Rotation about the z-axis changes $\widehat{H}_{so3}$
- $\boldsymbol{B}_{so}$ is then a function of the crystal axes as well as the dipole perturbation
  - This adjusts the previous structure
- We can explore the relative alignment of the crystal, dipole, and applied B-field
  - Fix dipole to original y-axis
  - Fix B-field to original x-axis
  - Rotate crystal axes

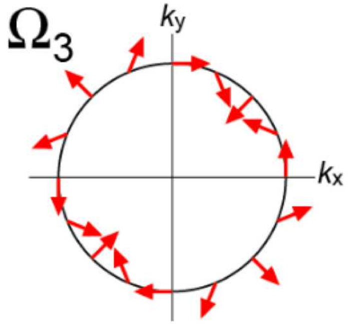

- Rotation of the spin-orbit field as a function of charge-carrier direction of motion for

$$\widehat{H}_{3,1} = i\alpha_{3,1}(\hat{\sigma}_- \otimes \hat{k}_+^3 - \hat{\sigma}_+ \otimes \hat{k}_-^3)$$

R. Moriya et al., PRL 2014

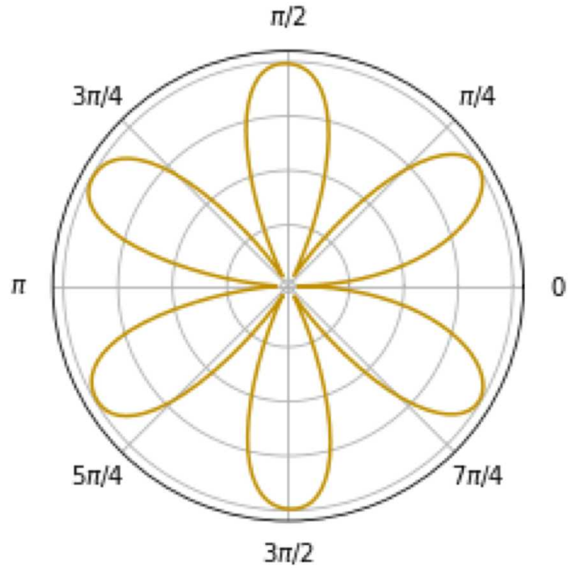

Future work

- Incorporate more microscopic details
  - QW band structure as a function of material conditions (effective masses)
  - Multi-band effective mass theory (light and heavy hole)
  - Static and dynamic noise sources
- Understand and optimize single-qubit gate fidelities
- Model two-qubit gate

Acknowledgements

Project PI: Dwight Luhman

Mentor: Andrew Baczewski

Experimentalists: Will Hardy, Tzu-Ming Lu

Theorists: Toby Jacobson, Leon Maurer

Sandia National Laboratories is a multi-missions laboratory managed and operated by National Technology and Engineering Solutions of Sandia, LLC, a wholly owned subsidiary of Honeywell International Inc., for DOE's National Nuclear Security Administration under contract DE-NA0003525.

Crystallographic axes relative to device design

- Form of $\hat{H}_{so3}$ imposes coordinate system
  - Crystal axes set by $\hat{k}_x$ and $\hat{k}_y$
  - Rotation about the z-axis changes $\hat{H}_{so3}$
- $\boldsymbol{B}_{so}$ is then a function of the crystal axes as well as the dipole perturbation
  - This adjusts the previous structure
- We can explore the relative alignment of the crystal, dipole, and applied B-field
  - Fix dipole to original y-axis
  - Rotate B-field
  - Rotate crystal axes

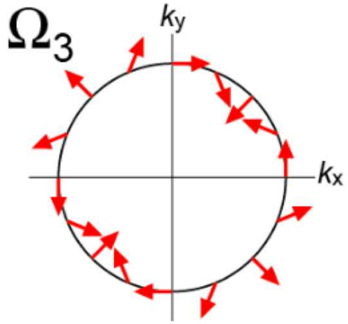

- Rotation of the spin-orbit field as a function of charge-carrier direction of motion for

$$\hat{H}_{3,1} = i\alpha_{3,1}\left(\hat{\sigma}_- \otimes \hat{k}_+^3 - \hat{\sigma}_+ \otimes \hat{k}_-^3\right)$$

R. Moriya et al., PRL 2014

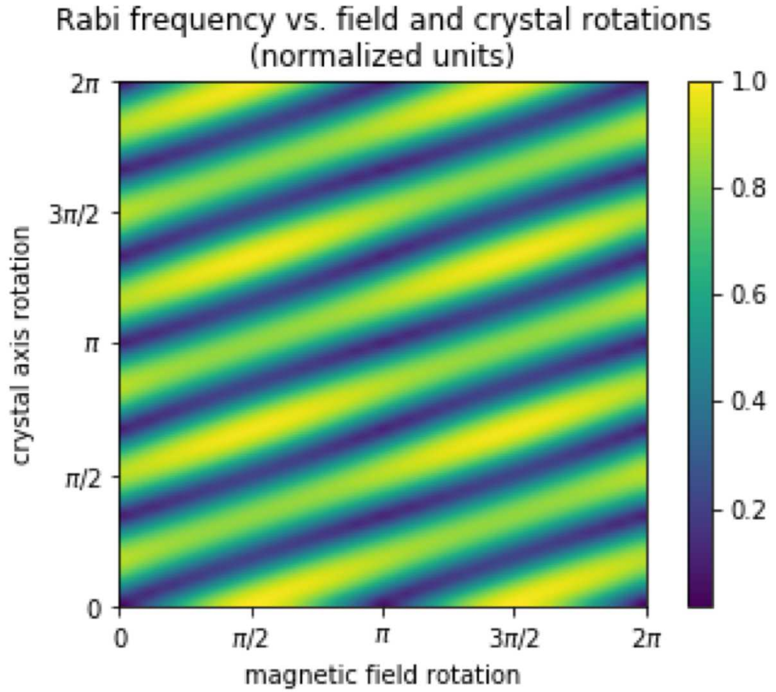

Qubit basis

- Without SOC:

$$|0\rangle = |\uparrow\rangle \otimes$$ 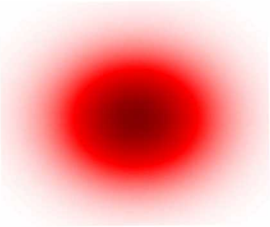

$$|1\rangle = |\downarrow\rangle \otimes$$ 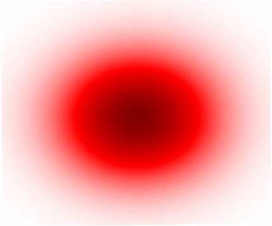

- With SOC:

$$|0\rangle = \alpha|\uparrow\rangle \otimes$$ 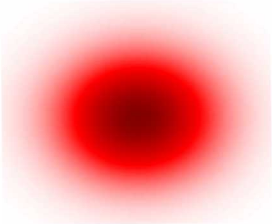

$$+\beta|\downarrow\rangle \otimes$$ 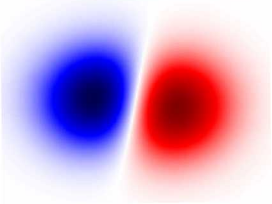

$$|1\rangle = \gamma|\uparrow\rangle \otimes$$ 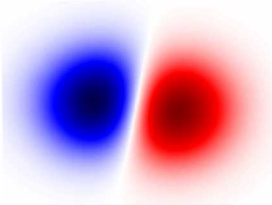

$$+\delta|\downarrow\rangle \otimes$$ 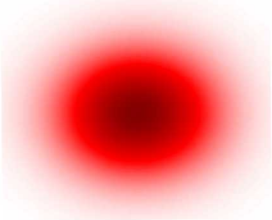

Linear SOC

- Hamiltonian:

$$\hat{H}_{so1} = i\alpha_1(\hat{\sigma}_- \otimes \hat{k}_+ - \hat{\sigma}_+ \otimes \hat{k}_-)$$

- Gate oscillation coupling:

$$\hat{D}_{ac} \sim V_{ac}\hat{y}$$

- Rabi frequency low when

$$\boldsymbol{B}_{app} \perp \hat{y}$$

in the xy-plane, high when

$$\boldsymbol{B}_{app} \parallel \hat{y}$$

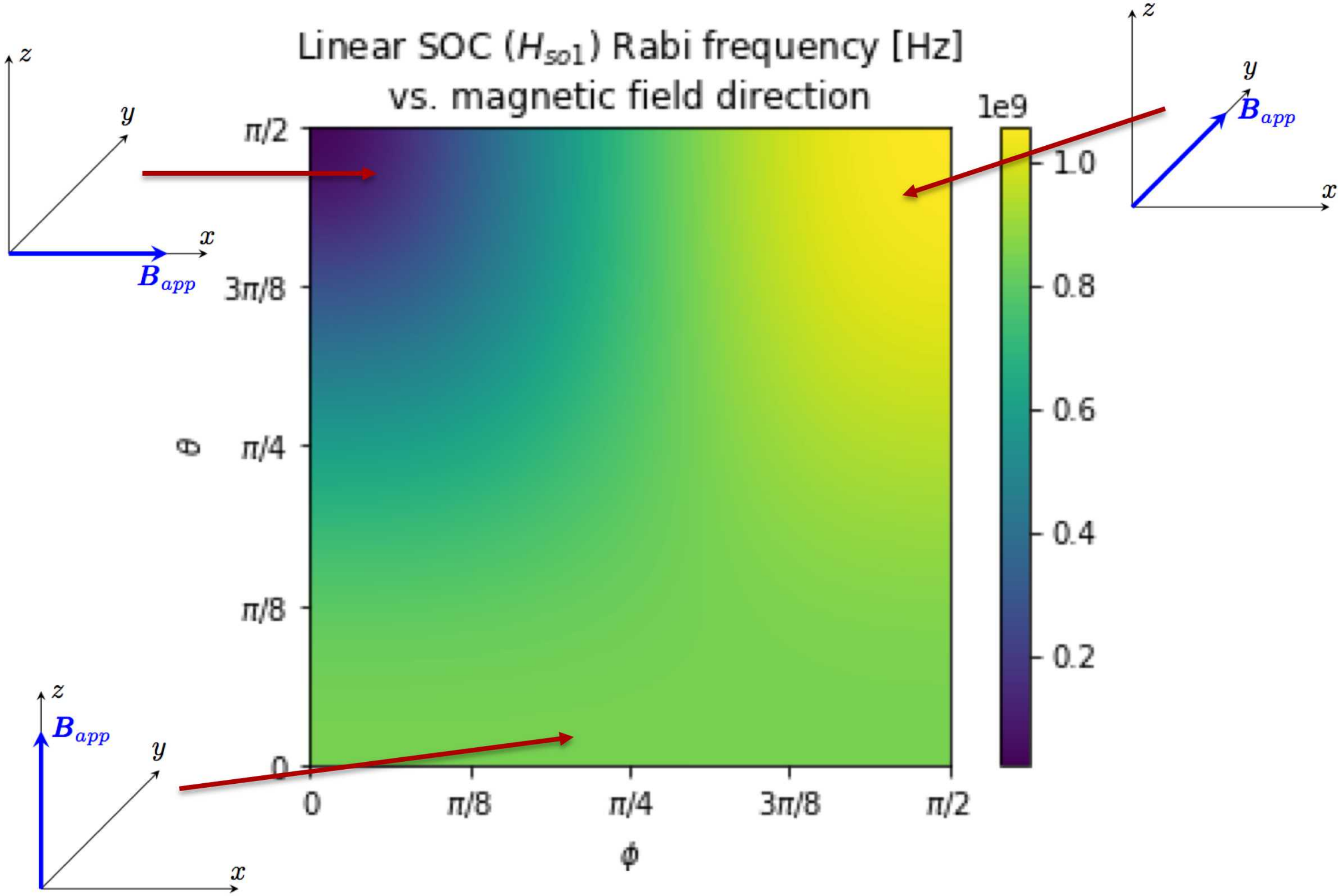

Cubic SOC

- Hamiltonian:

$$\hat{H}_{3,2} = i\alpha_{3,2}(\hat{\sigma}_- \otimes \hat{k}_-\hat{k}_+\hat{k}_- - \hat{\sigma}_+ \otimes \hat{k}_+\hat{k}_-\hat{k}_+)$$

- Gate oscillation coupling:

$$\hat{D}_{ac} \sim V_{ac}\hat{y}$$

- Similar qualities to linear for $\boldsymbol{B}_{app} \perp \hat{y}$ and $\boldsymbol{B}_{app} \parallel \hat{y}$ situations

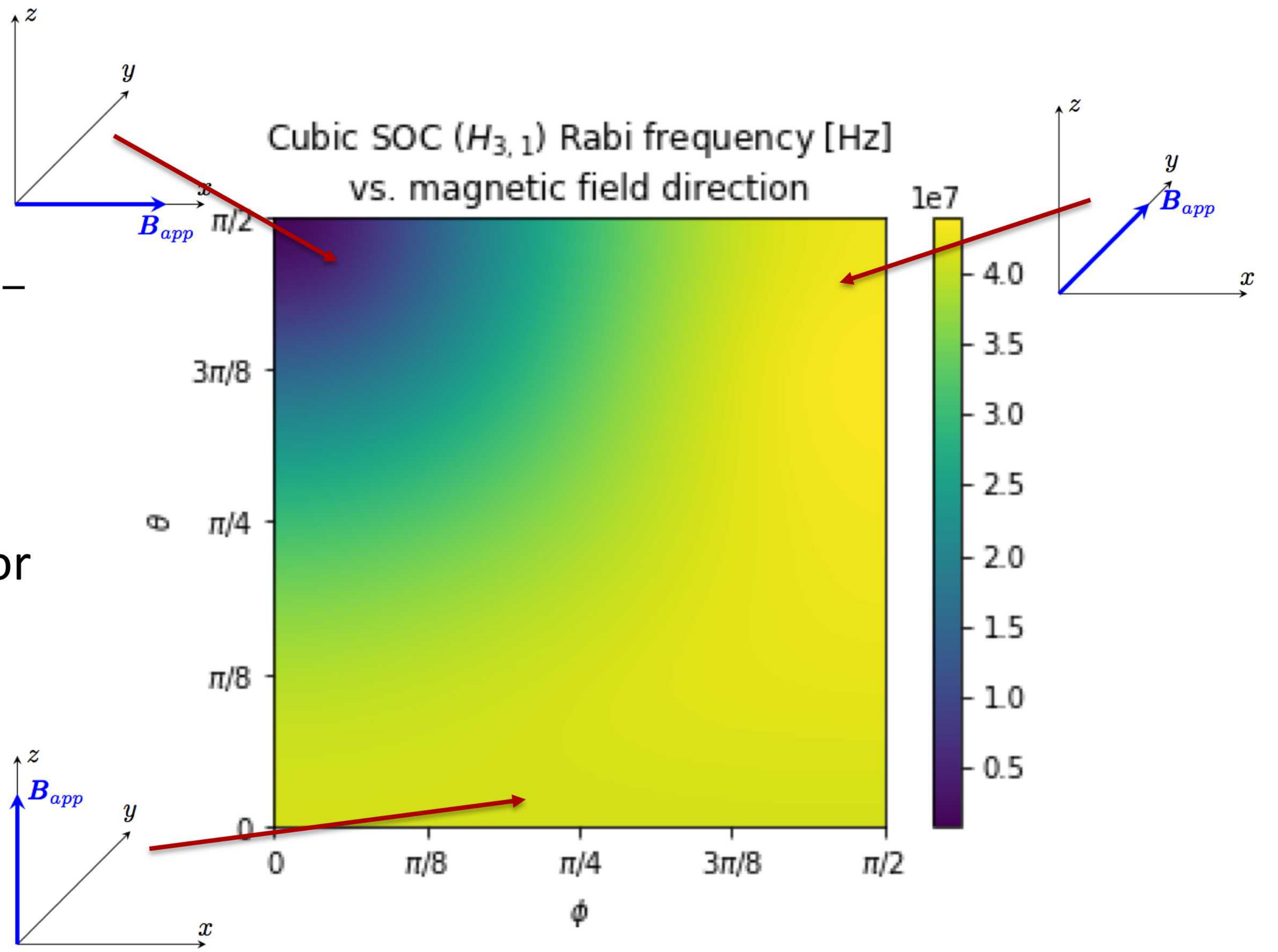

Understanding SOC trends

- $\hat{H}_{so1} = \alpha_1\left(\hat{\sigma}_y \otimes \hat{k}_x - \hat{\sigma}_x \otimes \hat{k}_y\right)$
- $\hat{H}_{3,1} \approx \alpha_{3,1}(\hat{\sigma}_y \otimes \left(\hat{k}_x^2 - 3\hat{k}_y^2\right)\hat{k}_x - \hat{\sigma}_x \otimes \left(\hat{k}_y^2 - 3\hat{k}_x^2\right)\hat{k}_y)$
- $\hat{H}_{3,2} \approx \alpha_{3,2}(\hat{\sigma}_y \otimes \left(\hat{k}_x^2 + \hat{k}_y^2\right)\hat{k}_x - \hat{\sigma}_x \otimes (\hat{k}_x^2 + \hat{k}_y^2)\hat{k}_y)$
- $\hat{D}_{ac} \sim V_{ac}\hat{y} \rightarrow k_x \sim 0 \rightarrow B_{so} \propto \hat{x}$

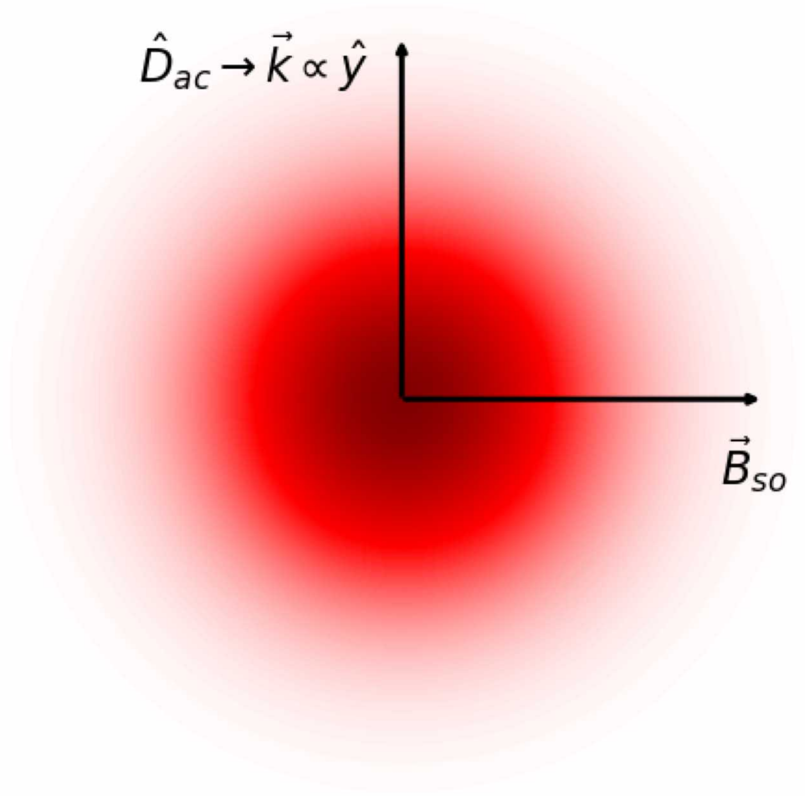

Understanding SOC trends

- $\hat{H}_{so1} \sim \hat{\sigma}_x \otimes \hat{k}_y$
- $\hat{H}_{3,1} \sim \hat{\sigma}_x \otimes \hat{k}_y^3$
- $\hat{H}_{3,2} \sim \hat{\sigma}_x \otimes \hat{k}_y^3$

- $\hat{D}_{ac} \sim V_{ac}\hat{y} \rightarrow k_x \sim 0 \rightarrow B_{so} \propto \hat{x}$